

## Supplementary Figures and Tables

### 1. Projected Density of States

The projected density of states for defect formation of  $\text{Y}_{\text{Ba}}$ ,  $\text{Y}_{\text{Fe}}$   $\text{Ce}_{\text{Ba}}$ , and  $\text{Ce}_{\text{Fe}}$  defects in BFO, shows similar trends to defect formation in  $\text{La}_{\text{Ba}}$  and  $\text{La}_{\text{Fe}}$  structures. Specifically,  $\text{A}_{\text{Ba}}$  defects are show a shift in the Fermi level of the O 2p states to higher energies, suggesting hole reduction  $\text{B}_{\text{Fe}}$  defects show little effect on O 2p states.

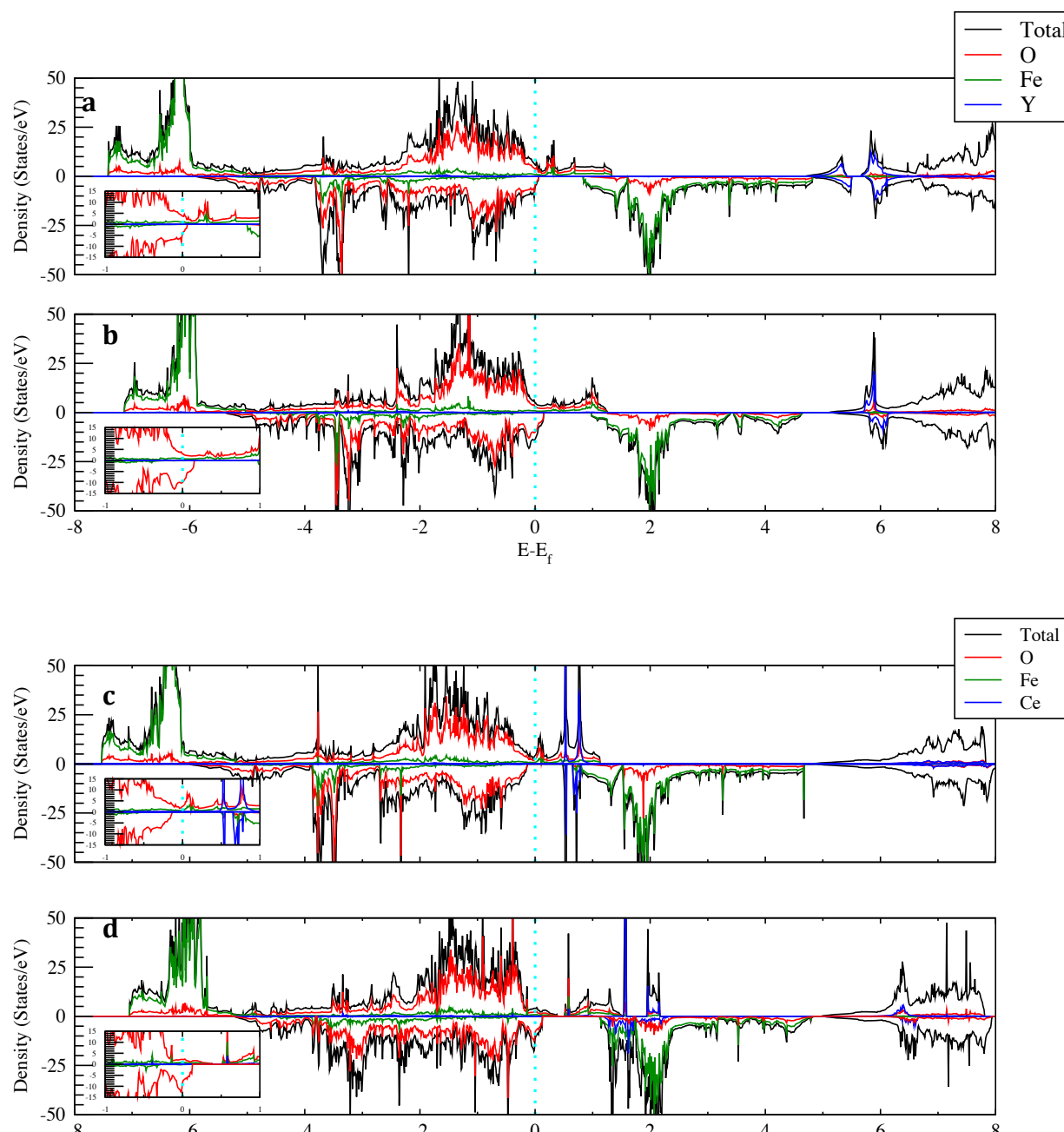


Figure S1 Projected Fe, O, Y & Ce, and total density of states of  $\text{BaFeO}_3$  with a)  $\text{Y}_{\text{Ba}}$ , b)  $\text{Y}_{\text{Fe}}$ , c)  $\text{Ce}_{\text{Ba}}$  and, d)  $\text{Ce}_{\text{Fe}}$  substitutions. The dashed cyan line corresponds to Fermi energy and insets show Fermi-level detail.

## 2. Bader Charge Analysis for Oxygen Vacancy formation

Bader charge analysis of oxygen vacancy formation for all  $\text{Ce}_{\text{Ba}}$ ,  $\text{Ce}_{\text{Fe}}$ ,  $\text{Y}_{\text{Ba}}$  and  $\text{Y}_{\text{Fe}}$  defects in BFO, shows a the same trend for charge redistribution with oxygen vacancy formation as observed for  $\text{La}_{\text{Ba}}$  and  $\text{La}_{\text{Fe}}$  structures. That is, a predominant localisation of additional charge to O sub-lattice for  $\text{B}_{\text{Fe}}$  defects, and significant localisation of dopant charge to A-manifold for  $\text{A}_{\text{Ba}}$  defects

Table S1. Bader charge  $q(e)$ , Magnetic moment of Fe  $\mu_{\text{Fe}}(\mu_B)$  for the stoichiometric structures of BFO and BFO with  $\text{Ce}_{\text{Ba}}$ ,  $\text{Ce}_{\text{Fe}}$ ,  $\text{Y}_{\text{Ba}}$  and  $\text{Y}_{\text{Fe}}$  defects.  $\delta=0$  corresponds to stoichiometric structure and  $\delta=0.125$  corresponds to a single oxygen vacancy. To note Bader chargers for oxygen vacancy structures, are for the optimum oxygen vacancy sites, as discussed in the manuscript.

Property	$\text{Ce}_{\text{Ba}}$		$\text{Ce}_{\text{Fe}}$		$\text{Y}_{\text{Ba}}$		$\text{Y}_{\text{Fe}}$	
	$\delta = 0$	$\delta = 0.125$	$\delta = 0$	$\delta = 0.125$	$\delta = 0$	$\delta = 0.125$	$\delta = 0$	$\delta = 0.125$
$\mu_{\text{Fe}}^{\text{a}}$	3.92	4.05	3.77	3.82	3.88	4.00	3.79	3.88
$\mu_{\text{Fe}^*}^{\text{a},\text{b}}$	---	3.81	---	3.85	---	3.74	---	3.54
$q_{\text{Fe}}^{\text{a}}$	1.83	1.82	1.74	1.76	1.83	1.79	1.70	1.75
$q_{\text{Fe}^*}^{\text{a},\text{b}}$	---	1.68	---	1.71	---	1.67	---	1.76
$q_{\text{Ba}}^{\text{a}}$	1.59	1.55	1.57	1.56	1.58	1.55	1.59	2.56
$q_{\text{A/B}}^{\text{a}}$	2.20	2.38	2.26	2.26	2.21	2.54	2.12	2.13
$q_{\text{o}}^{\text{a}}$	-1.16	-1.20	-1.12	-1.17	-1.17	-1.18	-1.11	-1.17

<sup>a</sup> To note Bader chargers for oxygen vacancy structures, are for the optimum oxygen vacancy sites, as discussed in the manuscript. <sup>b</sup>  $\text{Fe}^*$  indicates the Fe ions adjacent to the vacancy.